

for the lowest energy MLCT singlet and triplet excited levels and for the less negative reduction potentials. The luminescence and reduction properties are substantially those of the $\text{Ru}(\text{bpy})_2^{2+}$ unit, perturbed to a different degree in the monomer and dimer.

A detailed study of the temperature dependence of the luminescence (spectra and lifetimes) has allowed us to obtain a complete picture of the role played by the radiative and nonradiative transitions and to show that (i) the luminescent level of the monomer is much more sensitive to the environment than that of the dimer and (ii) the deactivation via the reactive ^3MC level can occur for the luminescent level of the dimer but not for that of the monomer. The latter conclusion is in full agreement with the photochemical results in $\text{CH}_2\text{Cl}_2/\text{Cl}^-$, which show that the monomer is photoinert whereas the dimer is strongly photosen-

sitive. Because of the nonequivalence of the coordinating positions of the bridging ligand, the luminescent excited state (namely, the lowest $^3\text{MLCT}$ level) and the reactive excited state (namely, the lowest ^3MC level) are localized on different Ru-containing units in the dinuclear complex 2.

Acknowledgment. We wish to thank L. Minghetti and G. Gubellini for technical assistance and Johnson and Matthey Chemical Ltd. (Reading, U.K.) for the generous loan of RuCl_3 . This work was supported by the Consiglio Nazionale delle Ricerche (Progetto Finalizzato Chimica Fine II) and the Ministero della Pubblica Istruzione.

Registry No. 1, 114397-51-2; 2, 114397-53-4; $\text{Ru}(\text{bpy})_2\text{Cl}_2$, 15746-57-3.

Contribution from the Dipartimento di Chimica, Centro di Fotochimica CNR, Università di Ferrara, 44100 Ferrara, Italy, and Dipartimento di Chimica "G. Ciamician", Università di Bologna, 40100 Bologna, Italy

Oligomeric Dicyanobis(polypyridine)ruthenium(II) Complexes. Synthesis and Spectroscopic and Photophysical Properties

C. A. Bignozzi,^{*1a} S. Roffia,^{1b} C. Chiorboli,^{1a} J. Davila,^{1a,c} M. T. Indelli,^{1a} and F. Scandola^{1a}

Received February 22, 1989

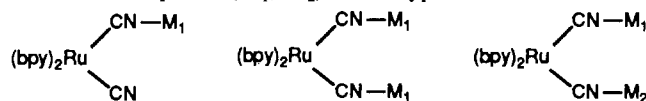
The polychromophoric systems $\text{NC-Ru}^{\text{II}}(\text{bpy})_2\text{-CN-Ru}^{\text{II}}(\text{bpy})_2\text{-CN}^+$ (2,2), $\text{NC-Ru}^{\text{II}}(\text{bpy})_2\text{-CN-Ru}^{\text{II}}(\text{phen})_2\text{-CN}^+$ (2,2'), and $\text{NC-Ru}^{\text{II}}(\text{bpy})_2\text{-CN-Ru}^{\text{II}}(\text{bpy})_2\text{-NC-Ru}^{\text{II}}(\text{bpy})_2\text{-CN}^{2+}$ (2,2,2) have been synthesized. Their redox, spectroscopic, and photophysical properties have been studied and compared with those of the $\text{Ru}(\text{bpy})_2(\text{CN})_2$ and $\text{Ru}(\text{phen})_2(\text{CN})_2$ complexes. In the series $\text{Ru}(\text{bpy})_2(\text{CN})_2$, (2,2), (2,2,2), $\text{Ru}(\text{phen})_2(\text{CN})_2$, and (2,2') the ease of oxidation of the ruthenium atoms increases in the order NC-Ru-CN , CN-Ru-CN , CN-Ru-NC . All the complexes were found to be emitting, with monoexponential decays of the emission intensity at 298 K as well as at 77 K. The energy of the emissions undergoes a bathochromic shift in going from mononuclear to polynuclear species, indicating that the lowest $d-\pi^*$ triplet excited state is on the N-bonded $\text{Ru}(\text{bpy})_2^{2+}$ or $\text{Ru}(\text{phen})_2^{2+}$ chromophoric unit and that intramolecular energy transfer between the C-bonded and N-bonded chromophores is very efficient. The singly oxidized forms of the polynuclear complexes $\text{NC-Ru}^{\text{III}}(\text{bpy})_2\text{-CN-Ru}^{\text{II}}(\text{bpy})_2\text{-CN}^{2+}$ (2,3), $\text{NC-Ru}^{\text{III}}(\text{bpy})_2\text{-CN-Ru}^{\text{III}}(\text{phen})_2\text{-CN}^{2+}$ (2,3'), and $\text{NC-Ru}^{\text{III}}(\text{bpy})_2\text{-CN-Ru}^{\text{III}}(\text{bpy})_2\text{-NC-Ru}^{\text{II}}(\text{bpy})_2\text{-CN}^{3+}$ (2,3,2) were electrochemically or chemically generated in D_2O solutions. The intense metal-to-metal ($\text{Ru}^{\text{II}} \rightarrow \text{Ru}^{\text{III}}$) IT transitions observed for the mixed-valence species in the near-infrared region indicate a high degree of electron delocalization relative to that of typical class II mixed-valence compounds. The lack of emission for (2,3), (2,3'), and (2,3,2) is assigned to highly efficient intramolecular electron-transfer quenching processes.

Introduction

There has been recently considerable interest in the synthesis and characterization of polynuclear transition-metal complexes in which a photosensitizer moiety is covalently bound to other moieties that can function as electron donors or acceptors²⁻¹¹ or as energy acceptors.¹²⁻¹⁷ The interest in this area is related to

the possibility to use coordination compounds as building blocks in the design of photochemical molecular devices.¹⁸

In this context, a number of adducts between the *cis*- $\text{Ru}(\text{bpy})_2(\text{CN})_2$ chromophore and solvated metal ions or transition-metal complexes (M_1 , M_2) of the type



have been synthesized and described in the last few years.^{9,10,14,19-26} Depending on the properties (excited-state energies, redox po-

- (1) (a) Università di Ferrara. (b) Università di Bologna. (c) Present address: Department of Physical Chemistry, Universidad Complutense, Madrid, Spain.
- (2) Creutz, C.; Kroger, P.; Matsubara, T.; Netzel, T. L.; Sutin, N. *J. Am. Chem. Soc.* **1979**, *101*, 5442.
- (3) Curtis, J. C.; Bernstein, J. S.; Meyer, T. J. *Inorg. Chem.* **1985**, *24*, 385.
- (4) Westmoreland, T. D.; Schanze, K. S.; Neveux, P. E., Jr.; Danielson, E.; Sullivan, B. P.; Chen, P.; Meyer, T. J. *Inorg. Chem.* **1985**, *24*, 2596.
- (5) Chen, P.; Westmoreland, T. D.; Danielson, E.; Schanze, K. S.; Anthon, D.; Neveux, P. E., Jr.; Meyer, T. J. *Inorg. Chem.* **1987**, *26*, 1116.
- (6) Danielson, E.; Elliott, C. M.; Merket, J. W.; Meyer, T. J. *J. Am. Chem. Soc.* **1987**, *109*, 2519.
- (7) Schanze, K. S.; Neyhart, G. A.; Meyer, T. J. *J. Phys. Chem.* **1986**, *90*, 2182.
- (8) Meyer, T. J. In *Supramolecular Photochemistry*; Balzani, V., Ed.; Reidel: Dordrecht, The Netherlands, 1987; p 103.
- (9) Bignozzi, C. A.; Roffia, S.; Scandola, F. *J. Am. Chem. Soc.* **1985**, *107*, 1644.
- (10) Bignozzi, C. A.; Paradisi, C.; Roffia, S.; Scandola, F. *Inorg. Chem.* **1988**, *27*, 408.
- (11) Katz, N. E.; Creutz, C.; Sutin, N. *Inorg. Chem.* **1988**, *27*, 1687.
- (12) Kane-Maguire, N. A. P.; Allen, M. M.; Vaught, J. M.; Hallock, J. S.; Heatherington, A. L. *Inorg. Chem.* **1983**, *22*, 3851.
- (13) Schmehl, R. H.; Auerbach, R. A.; Wacholtz, W. F.; Elliott, C. M.; Freitag, R. A.; Merket, J. W. *Inorg. Chem.* **1986**, *25*, 2440.
- (14) Endicott, J. F.; Lessard, R. B.; Ley, Y.; Ryu, C. K. In *Supramolecular Photochemistry*; Balzani, V., Ed.; Reidel: Dordrecht, The Netherlands, 1987; p 167.

- (15) Petersen, J. D. In *Supramolecular Photochemistry*; Balzani, V., Ed.; Reidel: Dordrecht, The Netherlands, 1987; p 135.
- (16) Furue, M.; Kinoshita, S.; Kushida, T. *Chem. Lett.* **1987**, 2355.
- (17) Bignozzi, C. A.; Indelli, M. T.; Scandola, F. *J. Am. Chem. Soc.* **1989**, *111*, 5192.
- (18) Balzani, V.; Moggi, L.; Scandola, F. In *Supramolecular Photochemistry*; Balzani, V., Ed.; Reidel: Dordrecht, The Netherlands, 1987; p 1.
- (19) Demas, J. N.; Addington, J. W.; Peterson, S. H.; Harris, E. W. *J. Phys. Chem.* **1977**, *81*, 1039.
- (20) Kinnaird, M. G.; Whitten, D. G. *Chem. Phys. Lett.* **1982**, *88*, 275.
- (21) Bartocci, C.; Bignozzi, C. A.; Scandola, F.; Rumin, R.; Courtot, P. *Inorg. Chim. Acta* **1983**, *76*, L 119.
- (22) Bignozzi, C. A.; Scandola, F. *Inorg. Chem.* **1984**, *23*, 1540.
- (23) Balzani, V.; Sabbatini, N.; Scandola, F. *Chem. Rev.* **1986**, *86*, 319.
- (24) Scandola, F.; Bignozzi, C. A.; Balzani, V. In *Homogeneous and Heterogeneous Photocatalysis*; Pelizzetti, E., Serpone, N., Eds.; D. Reidel: Dordrecht, The Netherlands, 1986; p 29.
- (25) Scandola, F.; Bignozzi, C. A. In *Supramolecular Photochemistry*; Balzani, V., Ed.; D. Reidel: Dordrecht, The Netherlands, 1987; p 121.
- (26) Scandola, F. In *Photochemical Energy Conversion*; Norris, J. R., Jr., Meisel, D., Eds.; Elsevier: New York, 1989; p 60.
- (27) Bignozzi, C. A.; Scandola, F. *Inorg. Chim. Acta* **1984**, *86*, 133.

tentials) of the M_1 , M_2 subunits, various types of effects have been observed in these polynuclear systems, going from perturbation of the $\text{Ru}(\text{bpy})_2(\text{CN})_2$ chromophore (blue shifts in the energy and changes in the lifetime of the $\text{Ru} \rightarrow \text{bpy}$ metal-to-ligand charge transfer (MLCT) triplet excited state),²³ to intramolecular quenching via energy-^{19,25} or electron-transfer^{9,10,25,26} processes.

Polynuclear cyano-bridged cationic species made of $\text{Ru}(\text{bpy})_2^{2+}$ units of the type $\text{NC}[\text{Ru}(\text{bpy})_2\text{CN}]_n\text{Ru}(\text{bpy})_2\text{CN}^{(2n+1)+}$ were obtained in the course of a previous study, as a nonresolvable polymeric mixture.²⁷ These species are potentially interesting from the point of view of electron or energy transport and of multielectron catalysis. The mixtures were characterized to some extent, with the understanding that the results represented average properties of oligomers of different chain lengths. Contrary to the general behavior observed for the other polynuclear complexes,^{20,22} these species exhibited an emission that was *red-shifted* with respect to that of the monomeric $\text{Ru}(\text{bpy})_2(\text{CN})_2$ complex. This fact suggested that the lowest $d-\pi^*$ triplet excited state could be that of the N-bonded $\text{Ru}(\text{bpy})_2^{2+}$ chromophore and that efficient intramolecular energy transfer between adjacent $\text{Ru}(\text{bpy})_2^{2+}$ units could be directed by the $-\text{CN}-$, $-\text{CN}-$ isomerism of the bridging ligands.

In order to investigate these aspects in some detail, we have now undertaken the synthesis of *discrete* cyano-bridged polynuclear species. We have succeeded in synthesizing the following binuclear and trinuclear species: $\text{NC}-\text{Ru}^{\text{II}}(\text{bpy})_2-\text{CN}-\text{Ru}^{\text{II}}(\text{bpy})_2-\text{CN}^+$, $\text{NC}-\text{Ru}^{\text{II}}(\text{bpy})_2-\text{CN}-\text{Ru}^{\text{II}}(\text{phen})_2-\text{CN}^+$, and $\text{NC}-\text{Ru}^{\text{II}}(\text{bpy})_2-\text{CN}-\text{Ru}^{\text{II}}(\text{bpy})_2-\text{CN}-\text{Ru}^{\text{II}}(\text{bpy})_2-\text{CN}-\text{Ru}^{\text{II}}(\text{bpy})_2-\text{CN}^{2+}$.

We report here on the spectroscopic, electrochemical, and photophysical properties of these new complexes and of their mixed-valence forms.

Experimental Section

Materials. The following commercially available chemicals were used without further purification: $\text{RuCl}_3 \cdot 3\text{H}_2\text{O}$ (Aldrich); NaN_3 , NaNO_2 , $(n\text{-C}_4\text{H}_9)_4\text{NClO}_4$ (Carlo Erba); $\text{Ce}(\text{NH}_4)_2(\text{NO}_3)_6$, NH_4PF_6 , $(\text{C}_4\text{H}_9)_4\text{N}-\text{CN}$, $(\text{C}_2\text{H}_5)_4\text{NBF}_4$ ([TEA]TfB), $(\text{C}_2\text{H}_5)_3\text{NCl}$ (Fluka). Spectrograde organic solvents, 70% HPF_6 (Aldrich), D_2O (Fluka), and tetradistilled water were used. Methanol was dried over 3-Å molecular sieves.

The chromatographic separations were made with neutral aluminium oxide, silica gel (Merck), Sephadex LH20, and Sephadex SP-C25-120 strongly acidic cationic-exchange resin (Pharmacia).

Preparations of Compounds. $\text{Ru}(\text{bpy})_2(\text{CN})_2$,²⁸ $\text{Ru}(\text{phen})_2(\text{CN})_2$,²⁹ $\text{Ru}(\text{bpy})_2\text{Cl}_2$,³⁰ $\text{Ru}(\text{bpy})_2(\text{NO}_2)_2$,³¹ $[\text{Ru}(\text{bpy})_2(\text{NO})(\text{NO}_2)](\text{PF}_6)_2$,³¹ $\text{Ru}(\text{phen})_2\text{Cl}_2$,³² $\text{Ru}(\text{phen})_2(\text{NO}_2)_2$,³¹ and $[\text{Ru}(\text{phen})_2(\text{NO})(\text{NO}_2)](\text{PF}_6)_2$ ³¹ were prepared following literature methods.

$\text{Ru}(\text{bpy})_2(\text{NO}_2)(\text{CN})$. This complex was prepared by the procedure described for the analogous $\text{Ru}(\text{bpy})_2(\text{NO}_2)(\text{X})$ ($\text{X} = \text{Cl}, \text{I}$),³³ with the following modifications. Anhydrous methanol was used instead of acetone to yield solutions of the solvent complex $\text{Ru}(\text{bpy})_2(\text{CH}_3\text{OH})(\text{NO}_2)^+$. A stoichiometric amount of $(\text{C}_4\text{H}_9)_4\text{N}-\text{CN}$ was then added to the solvent complex and the reaction mixture refluxed for 5 h. The solution was rotary evaporated to dryness. The solid was washed with stirring at room temperature with three 10-mL portions of CH_3CN (or CH_3COCH_3) and air-dried. The orange product was finally recrystallized from methanol; 65% yield. Anal. Calcd for $\text{Ru}(\text{bpy})_2(\text{NO}_2)(\text{CN}) \cdot \text{H}_2\text{O}$: C, 50.09; H, 3.60; N, 16.69. Found: C, 49.23; H, 3.61; N, 16.39.

$\text{Ru}(\text{phen})_2(\text{NO}_2)(\text{CN})$. The procedure was the same as for $\text{Ru}(\text{bpy})_2(\text{NO}_2)(\text{CN})$, except that in order to obtain a solution of $\text{Ru}(\text{phen})_2(\text{CH}_3\text{OH})(\text{NO}_2)^+$, $[\text{Ru}(\text{phen})_2(\text{NO})(\text{NO}_2)]\text{PF}_6$ ³¹ was used as the starting material. The orange product was obtained in 60% yield. Anal. Calcd for $\text{Ru}(\text{phen})_2(\text{NO}_2)(\text{CN})$: C, 56.28; H, 3.02; N, 15.75. Found: C, 55.86; H, 3.00; N, 15.64.

$[\text{Ru}(\text{bpy})_2(\text{NO})(\text{CN})](\text{PF}_6)_2$ and $[\text{Ru}(\text{phen})_2(\text{NO})(\text{CN})](\text{PF}_6)_2$. These complexes were prepared by starting from $\text{Ru}(\text{bpy})_2(\text{NO}_2)(\text{CN})$ and $\text{Ru}(\text{phen})_2(\text{NO}_2)(\text{CN})$, respectively, following the procedure and purification methods reported for $[\text{Ru}(\text{bpy})_2(\text{NO})(\text{NO}_2)](\text{PF}_6)_2$.³¹ The pale

yellow-green complexes were obtained in 90% yield. Anal. Calcd for $[\text{Ru}(\text{bpy})_2(\text{NO})(\text{CN})](\text{PF}_6)_2$: C, 33.21; H, 2.12; N, 11.06. Found: C, 33.09; H, 2.09; N, 10.74. Calcd for $[\text{Ru}(\text{phen})_2(\text{NO})(\text{CN})](\text{PF}_6)_2$: C, 37.18; H, 2.0; N, 10.41. Found: C, 36.52; H, 2.04; N, 10.20.

$[\text{NC}-\text{Ru}(\text{bpy})_2-\text{CN}-\text{Ru}(\text{bpy})_2-\text{CN}]\text{PF}_6$. A 0.209-g sample of $[\text{Ru}(\text{bpy})_2(\text{NO})(\text{CN})](\text{PF}_6)_2$ (2.75×10^{-4} mol) was suspended in 50 mL of anhydrous methanol and 0.018 g (2.75×10^{-4} mol) of NaN_3 , dissolved in 5 mL of methanol, was slowly added with stirring. The color of the solution turned from yellow to red brown. After 1.5 h the formation of the solvent complex was complete and the precipitated NaPF_6 was filtered off. $\text{Ru}(\text{bpy})_2(\text{CN})_2 \cdot 2\text{H}_2\text{O}$ (1.2 g, 2.38×10^{-3} mol) was previously dried at 110 °C and dissolved in 80 mL of boiling anhydrous methanol. The solution containing the solvent complex was then added to that containing the dicyano complex. The reaction mixture was refluxed for 4 h and rotary evaporated to dryness. The solid mixture was stirred in CH_3CN at room temperature and filtered. Most of the $\text{Ru}(\text{bpy})_2(\text{CN})_2$ excess was collected on the filter while the reaction products remained dissolved in CH_3CN . The filtered solution was concentrated to 10 mL and loaded on a 3×60 cm Sephadex LH20 column. Elution was continued with CH_3CN until the red-brown fraction containing the products was completely eluted, leaving a small red fraction containing the reactants at the top of the column. The eluted red-brown fraction was concentrated to 10 mL, and a saturated CH_3CN solution of $(\text{C}_2\text{H}_5)_4\text{NCl}$ was added dropwise until complete precipitation of the products as chloride salts occurred. The precipitate was filtered, washed with ether, and air-dried. At this stage of the purification, only oligomeric reaction products had to be separated. The precipitate was dissolved in water and loaded on a 3×20 cm Sephadex SP-C25-120 column. The red-orange dimeric complex was removed from the column with 0.2 M HCl. A brown byproduct was retained on the column. The eluted fraction was rotary evaporated to dryness and dissolved in water, and the product was precipitated as the hexafluorophosphate salt. The so-obtained red-brown solid was then dissolved in the minimum volume of hot water and reprecipitated by a small addition of solid NH_4PF_6 , filtered, washed with a few milliliters of water and dried under vacuum over CaCl_2 . Yield: 70%. Anal. Calcd for $[\text{NC}-\text{Ru}(\text{bpy})_2-\text{CN}-\text{Ru}(\text{bpy})_2-\text{CN}]\text{PF}_6 \cdot 2\text{H}_2\text{O}$: C, 47.55; H, 3.34; N, 14.18. Found: C, 47.02; H, 3.33; N, 13.91.

$[\text{NC}-\text{Ru}(\text{bpy})_2-\text{CN}-\text{Ru}(\text{phen})_2-\text{CN}]\text{PF}_6$. The procedure was the same as for $[\text{NC}-\text{Ru}(\text{bpy})_2-\text{CN}-\text{Ru}(\text{bpy})_2-\text{CN}]\text{PF}_6$ except that a freshly prepared solution of $[\text{Ru}(\text{phen})_2(\text{CH}_3\text{OH})(\text{CN})]\text{PF}_6$ in anhydrous methanol was used as the starting material. Yield: 60%. Anal. Calcd for $[\text{NC}-\text{Ru}(\text{bpy})_2-\text{CN}-\text{Ru}(\text{phen})_2-\text{CN}]\text{PF}_6 \cdot 2\text{H}_2\text{O}$: C, 49.78; H, 3.2; N, 13.58. Found: C, 50.04; H, 3.06; N, 13.68.

$[\text{NC}-\text{Ru}(\text{bpy})_2-\text{CN}-\text{Ru}(\text{bpy})_2-\text{NC}-\text{Ru}(\text{bpy})_2-\text{CN}](\text{PF}_6)_2$. A 0.2-g sample of $\text{Ru}(\text{bpy})_2\text{Cl}_2$ (4.13×10^{-4} mol) was dissolved in ca. 150 mL of boiling methanol, the solution was cooled at room temperature, and 0.17 g of AgClO_4 (8.2×10^{-4} mol) was added. The solution was stirred overnight at room temperature, and the precipitated AgCl was filtered off. This solution was slowly added to a solution containing 1.9 g (4.08×10^{-3} mol) of anhydrous $\text{Ru}(\text{bpy})_2(\text{CN})_2$ in ca. 150 mL of methanol. The solution was stirred at 50 °C for 2 h and then rotary evaporated to dryness. The perchlorate salt of the trinuclear complex was dissolved in CH_3CN and purified through gel filtration and ion-exchange chromatography as above described for the binuclear complexes. The trinuclear complex was removed from the cationic resin with 0.6 M HCl. The eluted fraction was rotary evaporated and twice redissolved and precipitated with solid NH_4PF_6 . The filtered brown solid was washed with water and dried under vacuum. Yield: 80%. Anal. Calcd for $[\text{NC}-\text{Ru}(\text{bpy})_2-\text{CN}-\text{Ru}(\text{bpy})_2-\text{NC}-\text{Ru}(\text{bpy})_2-\text{CN}](\text{PF}_6)_2 \cdot 2\text{H}_2\text{O}$: C, 46.02; H, 3.13; N, 13.40. Found: C, 45.58; H, 3.15; N, 12.98.

Singly Oxidized Forms of the Polynuclear Complexes. The singly oxidized forms of the binuclear and trinuclear complexes were prepared in water or D_2O solutions by two methods: (i) controlled-potential electrolysis and (ii) chemical oxidation with $(\text{NH}_4)_2\text{Ce}(\text{NO}_3)_6$ or Br_2 (acetonitrile solutions). The controlled-potential electrolyses were made over platinum electrodes in 1 or 0.2 cm thick spectrophotometric cells. These oxidations were carried out in 0.1 M [TEA]TfB in D_2O solutions at potentials about 100 mV more positive than the first $E_{1/2}$ (see Table II). After a charge corresponding to one electron per molecule had passed, a limiting spectrum was obtained. During the electrolysis, isosbestic points were maintained at 360, 400, and 592 nm ($2,2 \rightarrow 2,3$) (for the abbreviations, see the Results); 390 and 562 nm ($2,2' \rightarrow 2,3'$); and 380, 412, and 660 nm ($2,2,2 \rightarrow 2,3,2$), indicating complete conversion to stable, one-electron-oxidized products. The chemical oxidations were performed by adding small amounts of standard acetonitrile solutions of Ce^{IV} or Br_2 ($\epsilon = 183 \text{ M}^{-1} \text{ cm}^{-1}$ at 392 nm)^{34,35} to aqueous or D_2O solu-

(28) Demas, J. N.; Turner, T. F.; Crosby, G. A. *Inorg. Chem.* **1969**, *8*, 674.

(29) The complex was prepared in water solution by reaction of $\text{Ru}(\text{phen})_2\text{Cl}_2$ with a 30–40-fold excess of KCN and purified as reported for $\text{Ru}(\text{bpy})_2(\text{CN})_2$.²⁸

(30) Sullivan, B. P.; Salmon, D. J.; Meyer, T. J. *Inorg. Chem.* **1978**, *17*, 3334.

(31) Godwin, J. B.; Meyer, T. J. *Inorg. Chem.* **1971**, *10*, 471.

(32) The complex was prepared and purified by following the procedure reported by Sullivan³⁰ for the analogous $\text{Ru}(\text{bpy})_2\text{Cl}_2$.

(33) Adeyemi, S. A.; Miller, F. J.; Meyer, T. J. *Inorg. Chem.* **1972**, *11*, 994.

(34) Callahan, R. W.; Brown, G. M.; Meyer, T. J. *Inorg. Chem.* **1975**, *14*, 1443.

Table I. Vibrational Frequencies and Relative Intensities in the CN Stretch Region of the Mononuclear and Polynuclear Complexes^a

| complexes | $\nu_{\text{CN}},^b \text{ cm}^{-1}$ | |
|--|--------------------------------------|------------------------------|
| | terminal | bridged |
| Ru(bpy) ₂ (NO ₂)(CN) | 2078 vs | |
| [Ru(bpy) ₂ (NO)(CN)](PF ₆) ₂ | 2153 vw | |
| Ru(phen) ₂ (NO ₂)(CN) | 2073 vs | |
| [Ru(phen) ₂ (NO)(CN)](PF ₆) ₂ | 2158 vw | |
| Ru(bpy) ₂ (CN) ₂ | 2053 vs (10), 2067 vs (10) | |
| Ru(phen) ₂ (CN) ₂ | 2056 vs (10), 2068 vs (10) | |
| [NC-Ru(bpy) ₂ -CN-Ru(bpy) ₂ -CN](PF ₆) ₂ | 2069 vs (10) | 2098 vs (4) |
| [NC-Ru(bpy) ₂ -CN-Ru(phen) ₂ -CN](PF ₆) ₂ | 2069 vs (10) | 2098 vs (4) |
| [NC-Ru(bpy) ₂ -CN-Ru(bpy) ₂ -NC-Ru(bpy) ₂ -CN](PF ₆) ₂ | 2073 vs (10) | 2099 vs (8) |
| [NC-Ru(bpy) ₂ -CN-Pt(dien)](ClO ₄) ₂ | 2058 vs (8.5) | 2108 vs (10) |
| [(dien)Pt-NC-Ru(bpy) ₂ -CN-Pt(dien)](ClO ₄) ₄ | | 2108 vs (10), 2129 vs (8) |

^a In KBr pellets; $\pm 4 \text{ cm}^{-1}$. ^b Abbreviations: very strong, vs; very weak, vw. Relative intensity is given in parentheses.

tions of the complexes. After addition of 1 equiv of oxidant, a limiting spectrum was reached. The limiting spectra and the isosbestic points observed during the chemical oxidation coincided with those obtained upon electrochemical oxidation.

When the oxidation of the polynuclear complexes was performed in CH₃CN solutions, isosbestic points were not maintained except for the initial stages, indicating some instability of the monooxidized forms, with concomitant release of Ru(bpy)₂(CN)₂ in this solvent.

Apparatus. Absorption spectra in the UV-vis/near-IR regions were taken with a Perkin-Elmer 323 spectrophotometer. Infrared spectra were recorded on KBr pellets with a Perkin-Elmer 283 spectrophotometer. Emission spectra were recorded with a Perkin-Elmer MPF 44E spectrofluorimeter equipped with a R928 Hamamatsu tube. All the emission spectra were corrected by calibrating the instrumental response with respect to a NBS standard quartz tungsten-halogen lamp.

The emission lifetimes were measured with a J&K System 2000 ruby laser (frequency-doubled, pulse half-width of 20 ns) in a single-shot mode with oscillographic recording, or with a PRA System 3000 nanosecond fluorescence spectrometer equipped with a Model 510B nanosecond pulsed lamp and a Model 1551 cooled photomultiplier; the data were collected on a Tracor-Northern 1750 multichannel analyzer and were processed on a Digital PDP 11/03 computer using original PRA software. Low-temperature emission spectra and lifetimes were measured by using Oxford Instruments DN 704 cryostatic equipment with quartz windows and 1-cm/spectrofluorimetric cuvettes.

The electrochemical measurements were taken in water, D₂O, CH₃CN, and DMF. The last two solvents were purified and dried with standard methods. Fluka reagent grade 0.1 M [TEA]TFB was used as the supporting electrolyte. All measurements were performed at 25 \pm 1 $^{\circ}\text{C}$.

Cyclic voltammetric (CV) measurements were carried out with an AMEL 552 potentiostat, an AMEL 568 programmable function generator, an AMEL Model 863 X/Y recorder and a Nicolet Model 3091 digital oscilloscope. The minimization of the uncompensated resistance effect in CV was achieved with a positive feedback network of the potentiostat. A conventional three-electrode cell was used in CV. A saturated calomel electrode, separated from test solution by a frit, was used as a reference electrode, and all potentials are referred to it. A hanging mercury drop electrode and a stationary platinum electrode were used as working electrodes.

Spectroelectrochemical experiments were carried out in an OTTLE (optical transparent thin-layer electrode) made of a 90% platinum-10% rhodium grid (Johnson Matthey) placed between the window of a 2-mm spectrophotometric cell directly mounted on a Perkin-Elmer 323 spectrophotometer. The counter electrode was a Pt wire separated from the cathodic compartment by a frit; an Ag wire was used as the reference electrode.

The charge exchanged during controlled-potential electrolytic experiments (CPE) was determined with an AMEL Model 731 integrator by using an apparatus essentially constituted by a conventional 1 cm spectrophotometric cell with a thin-plate Pt working electrode, a Pt-wire counter electrode and a Luggin capillary in contact with an SCE reference electrode.

Conductivity measurements were taken in CH₃CN at 25 \pm 1 $^{\circ}\text{C}$ with an Amel Model 133 conductivity meter.

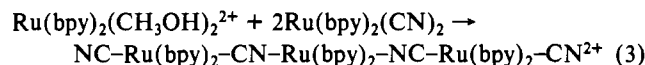
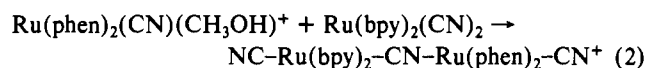
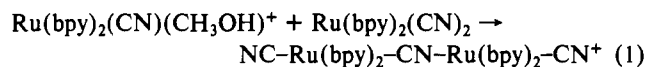
Results

For the sake of conciseness, abbreviations will be used in the Results and Discussion sections for the various polynuclear complexes, for example, NC-Ru^{II}(bpy)₂-CN-Ru^{II}(bpy)₂-CN⁺ (2,2), NC-Ru^{II}(bpy)₂-CN-Ru^{II}(phen)₂-CN⁺ (2,2'), and NC-Ru^{II}(bpy)₂-CN-Ru^{II}(bpy)₂-NC-Ru^{II}(bpy)₂-CN²⁺ (2,2,2).

The symbols in parentheses refer to the oxidation state of the various metal centers. Thus, abbreviations for oxidized species can be obtained from those given above by substitution of the "2" symbol with a "3" in the appropriate ruthenium center.

Synthesis and Characterization of the Polynuclear Complexes. The general synthetic strategy has been largely inspired by the work of Meyer on pyrazine-bridged oligomeric Ru(II) complexes.³⁶

The mononuclear complexes Ru(bpy)₂(CN)(X)ⁿ⁺ and Ru(phen)₂(CN)(X)ⁿ⁺ ($n = 0$, X = NO₂; $n = 2$, X = NO) were prepared by following the general method described by Meyer and co-workers for the synthesis of mixed cis ruthenium complexes.^{31,33} As shown by Meyer, the weakly bound solvent molecule (S), like CH₃COCH₃ or CH₃OH, in a complex of the type Ru(bpy)₂(S)(X) can easily be replaced with many other ligands, Y, giving the mixed Ru(bpy)₂(Y)(X) complex. The lability of the solvent molecule coordinated to ruthenium was exploited in reactions 1-3 to prepare the desired binuclear and trinuclear complexes.



Reactions 1-3 were carried out with a 10-fold excess of Ru(bpy)₂(CN)₂ to minimize the formation of polymeric species. The products of reactions 1-3 have been characterized, in addition to elemental analysis (see previous section), by various experimental techniques as described below.

Conductivity. The charge and molecular complexity of a cationic species can be established by comparing (at the same temperature and in the same solvent) the slope of an experimental plot of $(\Lambda_0 - \Lambda_c)$ vs $\sqrt{C_e}$ for solutions containing the investigated complex, with that obtained with a standard electrolyte containing the same anion or anions of similar Λ_0 .³⁷⁻⁴⁰ In the above equation, Λ_c and Λ_0 are the equivalent conductivity and the conductivity at infinite dilution respectively, and C_e is the equivalent concentration that can be derived from elemental analysis data. In Figure 1 are shown plots of $(\Lambda_0 - \Lambda_c)$ vs $\sqrt{C_e}$ for the binuclear and trinuclear complexes, for Ru(bpy)₃(PF₆)₂, a standard 2:1 electrolyte, and for (*n*-C₄H₉)₄NClO₄, a standard 1:1 electrolyte. The last compound can be used as a reference 1:1 electrolyte since the ClO₄⁻ and PF₆⁻ ions have, in CH₃CN solutions, comparable limiting conductivities ($\Lambda_0 = 103.4 \text{ mho}$ for ClO₄⁻; $\Lambda_0 = 102.8 \text{ mho}$ for PF₆⁻).³⁸

The experimentally determined slopes (mho L^{1/2} equiv^{-1/2}) were as follows: [NC-Ru(bpy)₂-CN-Ru(bpy)₂-CN]PF₆, 750 \pm 20; [NC-Ru(bpy)₂-CN-Ru(phen)₂-CN]PF₆, 690 \pm 20; [NC-Ru(bpy)₂-CN-Ru(bpy)₂-NC-Ru(bpy)₂-CN](PF₆)₂, 1180 \pm 20; (*n*-C₄H₉)₄NClO₄, 700 \pm 10; Ru(bpy)₃(PF₆)₂, 1060 \pm 20. Linear plots (not reported in Figure 1) were also obtained with [Ru(bpy)₃](ClO₄)₂ and [NC-Ru(bpy)₂-CN-Ru(bpy)₂-NC-Ru(bpy)₂-CN](ClO₄)₂ with slopes of 1020 and 1030. The very

(36) Adeyemi, S. A.; Johnson, E. C.; Miller, F. J.; Meyer, T. J. *Inorg. Chem.* **1973**, *12*, 2371.

(37) Feltham, R. D.; Hayter, R. G. *J. Chem. Soc.* **1964**, 4587.

(38) Boggess, R. K.; Zatko, D. A. *J. Chem. Educ.* **1975**, *52*, 649.

(39) Weaver, T. R.; Meyer, T. J.; Adeyemi, S. A.; Brown, G. M.; Eckberg, R. P.; Hatfield, W. E.; Johnson, E. C.; Murray, R. W.; Untereker, D. *J. Am. Chem. Soc.* **1975**, *97*, 3039.

(40) Rillema, D. P.; Callahan, R. W.; Mack, K. B. *Inorg. Chem.* **1982**, *21*, 2589.

(35) Powers, M. J.; Callahan, R. W.; Salmon, D. J.; Meyer, T. J. *Inorg. Chem.* **1976**, *15*, 894.

Table II. Ground and Excited-State Redox Potentials of Mononuclear and Polynuclear Complexes^a

| complexes | $E_{1/2}^{ox}, V$ | | | $E_{1/2}^{red(1)}, V$ ^c | E_{0-0}, eV ^d | $*E_{1/2}^{ox}, eV$ ^e | $*E_{1/2}^{red}, eV$ ^e |
|--|--------------------------------|-------------------|-------------------|------------------------------------|----------------------------|----------------------------------|-----------------------------------|
| | $E_{1/2}^{ox(1)}$ ^b | $E_{1/2}^{ox(2)}$ | $E_{1/2}^{ox(3)}$ | | | | |
| Ru(bpy) ₂ (CN) ₂ | +0.86 (+0.9) | | | -1.60 | 2.11 | -1.25 | +0.51 |
| Ru(phen) ₂ (CN) ₂ | +0.88 | | | -1.62 | 2.18 | -1.30 | +0.56 |
| [NC-Ru(bpy) ₂ -CN-Ru(bpy) ₂ -CN]PF ₆ | +0.74 (+0.64) | +1.35 | | -1.54 | 1.97 | -1.23 | +0.43 |
| [NC-Ru(bpy) ₂ -CN-Ru(phen) ₂ -CN]PF ₆ | +0.75 (+0.64) | +1.34 | | -1.54 | 2.00 | -1.25 | +0.46 |
| [NC-Ru(bpy) ₂ -CN-Ru(bpy) ₂ -NC-Ru(bpy) ₂ -CN](PF ₆) ₂ | +0.66 (+0.53) | +1.19 | +1.46 | -1.51 | 1.81 | -1.15 | +0.30 |

^aData in CH₃CN, Pt working electrode (vs SCE), unless otherwise noted. ^bData in parentheses refer to oxidation potentials determined in H₂O, Pt working electrode (vs SCE). ^cData in DMF, HME working electrode (vs SCE). ^dExcited-state energy, estimated from 77 K emission spectra. ^eEstimated from the relationships, $*E_{1/2}^{ox} \approx E_{1/2}^{ox(1)} - E_{0-0}$ and $*E_{1/2}^{red} \approx E_{1/2}^{red(1)} + E_{0-0}$.

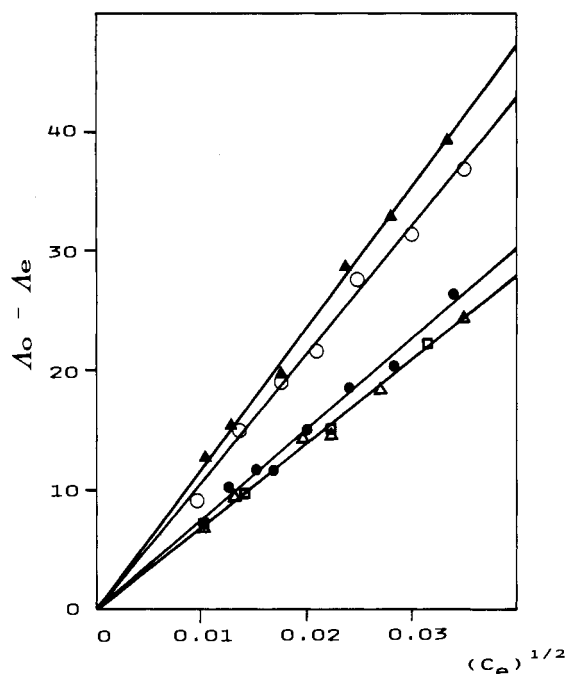


Figure 1. Plots of $(\Delta_0 - \Delta_2)$ vs $(C_e)^{1/2}$ from conductivity data in CH₃CN at 25 °C for $(n-C_4H_9)_4NClO_4$ (□), Ru(bpy)₃(PF₆)₂ (○), [NC-Ru(bpy)₂-CN-Ru(bpy)₂-CN](PF₆) (●), [NC-Ru(bpy)₂-CN-Ru(phen)₂-CN](PF₆) (▲), [NC-Ru(bpy)₂-CN-Ru(bpy)₂-NC-Ru(bpy)₂-CN](PF₆)₂ (▲).

similar slopes obtained for the standard 1:1 electrolyte and the binuclear complexes and for the standard 2:1 electrolyte and the trinuclear complex confirm the hypothesis about the ion type formulated for the different polynuclear cationic complexes.

Infrared Spectra. The infrared absorption bands of Ru(bpy)₂(NO₂)(CN) and Ru(phen)₂(NO₂)(CN) match very closely those reported for the analogous complexes of the type Ru(A-A)(NO₂)(X) (X = Cl, I, py, NO₂; A-A = bpy, phen).^{31,33} The complexes contain only the nitro (N-bonded) linkage isomer as shown by the absence of the stretching vibration due to oxygen-bonded nitrite in the 1130–1134- and 1394–1397-cm⁻¹ intervals. The very strong bands at 1295 and 1333 cm⁻¹ and 1290 and 1330 cm⁻¹, respectively, exhibited by Ru(bpy)₂(NO₂)(CN) and Ru(phen)₂(NO₂)(CN) can be confidently assigned to the symmetric and antisymmetric N–O stretching vibrations of the nitrogen-bonded –NO₂.^{31,33} The nitrosyl complexes [Ru(bpy)₂(NO)(CN)](PF₆)₂ and [Ru(phen)₂(NO)(CN)](PF₆)₂ show a very strong $\nu(N-O)$ band at 1950 cm⁻¹ and a very weak, barely detectable $\nu(C-N)$ band at 2153 and 2158 cm⁻¹, respectively. The high energy and the low intensity of the CN stretching vibrations in these complexes are not unexpected, since similar effects have been previously considered and discussed by other authors.^{41,42} The well-known ability of the NO⁺ ligand in delocalizing charge through $d\pi \rightarrow p\pi^*$ back-donation^{31,43,44} and the consequent de-

crease of the electron density on ruthenium should account for both effects.

The polynuclear (2,2), (2,2'), and (2,2,2) species exhibit all the bpy and phen bands that are expected as a superposition of the spectra of the monomeric units.

Relevant to the proposed structures of the polynuclear species (see Discussion) are the observed frequencies and the relative intensity in the doublets due to the CN stretching vibrations. These values are reported with those of the mononuclear complexes in Table I.

Electrochemistry. The electrochemistry of the binuclear and trinuclear complexes has been studied at room temperature by cyclic voltammetry and controlled-potential coulometry in CH₃CN, DMF, and D₂O solutions. The relevant electrochemical results are reported in Table II together with those for the *cis*-Ru(bpy)₂(CN)₂ and *cis*-Ru(phen)₂(CN)₂ complexes.^{45,46} The binuclear and trinuclear complexes exhibit two and three [Ru(II)/Ru(III)] oxidation waves, respectively, which correspond, on the basis of usual criteria,⁴⁷ to one-electron reversible processes. Several reduction steps were observed in the CV curves recorded, in DMF solutions of the polynuclear complexes, between –1.5 and –2.5 V. The use of simulation techniques⁴⁸ and the convolutive analysis of the voltammetric peaks⁴⁹ indicated the presence for the binuclear species of two doublets of closely lying one-electron reversible processes and of two triplets of closely lying one-electron reversible processes for the trinuclear complex.^{50–53} The values of the first reduction potentials are reported in Table II.

UV-Vis/Near-IR Absorption Spectra. Acetonitrile solutions of Ru(bpy)₂(CN)₂, (2,2), and (2,2,2) have similar absorption spectra (Figure 2). The UV region is dominated by $\pi-\pi^*$ transitions of the bpy ligands, and the visible region consists of MLCT ($d-\pi^*$) transitions characteristic of the Ru(bpy)₂²⁺ chromophoric unit.

The spectrum of the (2,2') complex, shown in Figure 3, exhibits a more structured absorption in the UV region, due to the presence

(41) Jones, L. H. *Inorg. Chem.* **1963**, *2*, 777.

(42) Schilt, A. A. *Inorg. Chem.* **1964**, *3*, 1323.

(43) Shriver, D. F.; Posner, J. J. *Am. Chem. Soc.* **1966**, *88*, 1672 and references therein.

(44) Johnson, B. F. G.; McCleverty, J. A. *Prog. Inorg. Chem.* **1966**, *7*, 277.

(45) The redox potentials reported in Table II, have not been corrected for the liquid-junction potential (ljp) between nonaqueous and aqueous solutions. The corrected redox potentials in acetonitrile solutions can be obtained from those reported in Table II by subtracting the ljp contribution, which can be estimated to be on the order of 0.19–0.15 V.⁴⁶

(46) Headridge, J. B. *Electrochemical Techniques for Inorganic Chemists*; Academic Press: New York, 1969.

(47) Nicholson, R. S.; Shain, I. *Anal. Chem.* **1964**, *36*, 706.

(48) Feldberg, S. W. In *Computer in Chemistry and Instrumentation*; Mattson, J. S., Mark, H. B., MacDonald, H. C., Eds.; Marcel Dekker: New York, 1969; Vol. 2, p 199.

(49) Ammar, F.; Savéant, J. M. *J. Electroanal. Chem. Interfacial Electrochem.* **1973**, *47*, 215.

(50) The number of one-electron reductive processes is in agreement with the formulation given for the bi- and trinuclear complexes. It is known in fact that the redox orbitals involved in the reductions of the –Ru(bpy)₂ and –Ru(phen)₂ units have a large bpy or phen π^* orbital character.^{51,52} Work is in progress at low temperature and in strictly aprotic conditions in order to observe the maximum extension of the ligand redox series⁵³ in the polynuclear complexes.

(51) Roffia, S.; Ciano, M. *J. Electroanal. Chem. Interfacial Electrochem.* **1977**, *77*, 349.

(52) De Armond, M. K.; Hanck, K. W.; Wertz, D. W. *Coord. Chem. Rev.* **1985**, *64*, 65.

(53) Vlček, A. A. *Coord. Chem. Rev.* **1982**, *43*, 39.

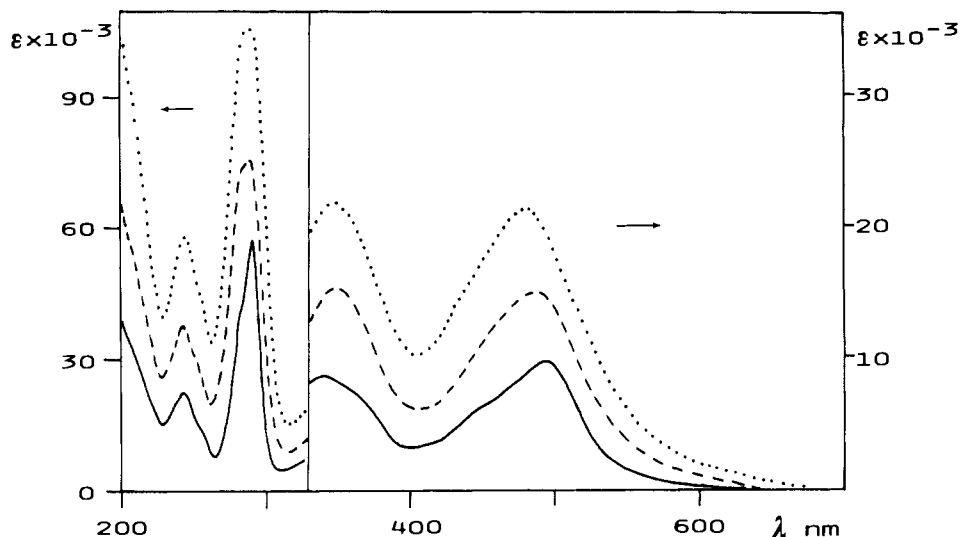


Figure 2. UV-visible spectra of $\text{Ru}(\text{bpy})_2(\text{CN})_2$ (—), $[\text{NC-Ru}(\text{bpy})_2\text{-CN-Ru}(\text{bpy})_2\text{-CN}](\text{PF}_6)$ (---), and $[\text{NC-Ru}(\text{bpy})_2\text{-CN-Ru}(\text{bpy})_2\text{-NC-Ru}(\text{bpy})_2\text{-CN}](\text{PF}_6)_2$ (···) in CH_3CN solutions.

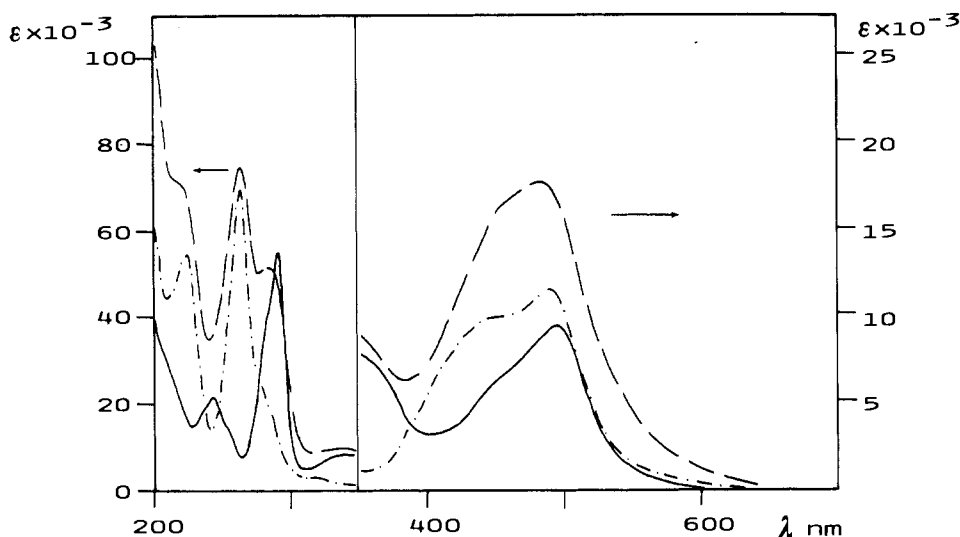


Figure 3. UV-visible spectra of $\text{Ru}(\text{phen})_2(\text{CN})_2$ (---), $\text{Ru}(\text{bpy})_2(\text{CN})_2$ (—) and $[\text{NC-Ru}(\text{bpy})_2\text{-CN-Ru}(\text{phen})_2\text{-CN}](\text{PF}_6)$ (— · —) in CH_3CN solutions.

Table III. Photophysical Properties of Mononuclear and Polynuclear Complexes

| complexes | $\bar{\nu}_{\text{max}}^{\text{em}}(298 \text{ K}),^a$ μm^{-1} | $\tau(298 \text{ K}),^a$ ns | $\bar{\nu}_{\text{max}}^{\text{em}}(77 \text{ K}),^b$ μm^{-1} | $\tau(77 \text{ K}),^b$ μs |
|---|--|--------------------------------|---|--|
| $\text{Ru}(\text{bpy})_2(\text{CN})_2$ | 1.45 | 240 | 1.70 | 4.0 |
| $\text{Ru}(\text{phen})_2(\text{CN})_2$ | 1.49 | 950 | 1.76 | 12.5 |
| $[\text{NC-Ru}(\text{bpy})_2\text{-CN-Ru}(\text{bpy})_2\text{-CN}]\text{PF}_6$ | 1.40 | 90 | 1.59 | 1.6 |
| $[\text{NC-Ru}(\text{bpy})_2\text{-CN-Ru}(\text{phen})_2\text{-CN}]\text{PF}_6$ | 1.43 | 400 | 1.70 | 4.6 |
| $[\text{NC-Ru}(\text{bpy})_2\text{-CN-Ru}(\text{bpy})_2\text{-NC-Ru}(\text{bpy})_2\text{-CN}](\text{PF}_6)_2$ | 1.36 | 50 | 1.46 | 1.3 |

^a In CH_3CN solutions. The lifetimes were determined in deaerated solutions. ^b In an absolute ethanol glass.

of $\pi-\pi^*$ transitions localized on the bpy and phen ligands. These transitions can be straightforwardly assigned by comparison with the absorption spectra of the $\text{Ru}(\text{bpy})_2(\text{CN})_2$ and $\text{Ru}(\text{phen})_2(\text{CN})_2$ complexes also reported in Figure 3. The absorption bands in the visible region arise from the MLCT ($d-\pi^*$) transitions of the $\text{Ru}(\text{bpy})_2^{2+}$ and $\text{Ru}(\text{phen})_2^{2+}$ moieties.

All these complexes exhibit solvent-dependent absorption spectra in the visible region, with blue shifts of the absorption maxima of the order of $0.3 \mu\text{m}^{-1}$ for $\text{Ru}(\text{bpy})_2(\text{CN})_2$ and $\text{Ru}(\text{phen})_2(\text{CN})_2$ and $0.2 \mu\text{m}^{-1}$ for the polynuclear complexes, in going from acetonitrile to water (see Figures 2 and 3 vs Figure 4). As previously noted for related systems, donor-acceptor interactions between the terminal cyanide groups and the solvent are responsible for the observed behavior.^{22,23,54-56}

The spectra of the electrochemically produced (2,3), (2,3'), and (2,3,2) complexes in D_2O solutions (for the assignment of the oxidation site, see Discussion) are compared in Figure 4 with those of the respective reduced forms. With oxidation, the intensity of the $\text{Ru}(\text{II}) \rightarrow \text{bpy}$ MLCT bands decreases and their maxima shift to the blue. Furthermore, a new band appeared in the near-IR region. This new band can be assigned to an intervalence-transfer (IT) transition between $\text{Ru}(\text{II})$ and $\text{Ru}(\text{III})$ centers (see Discussion).

Photophysical Properties. The (2,2), (2,2'), and (2,2,2) complexes are luminescent at room temperature as well as at 77 K, with strictly monoexponential decays of the emission intensity.

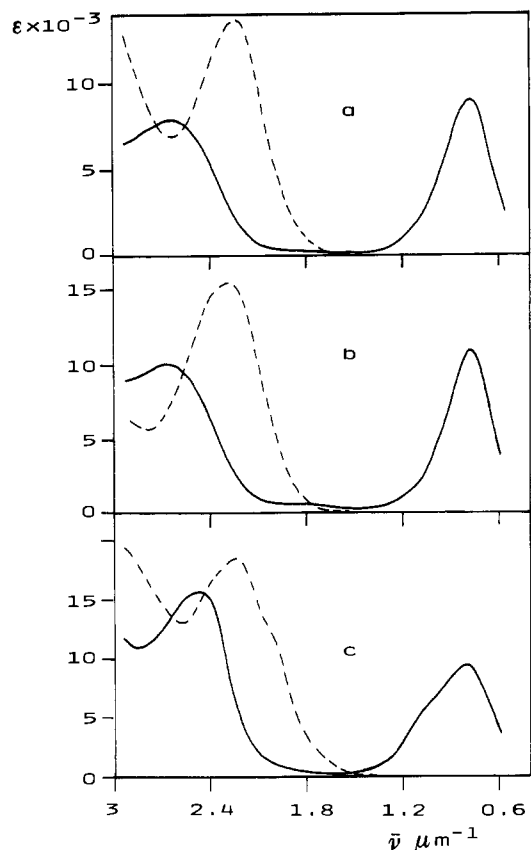


Figure 4. UV-visible and near-IR spectra in D_2O solutions: (a) (2,2) (---), (2,3) (—); (b) (2,2') (---), (2,3') (—); (c) (2,2,2) (---), (2,3,2) (—). For the abbreviations see text.

The lifetimes and the maxima of the room temperature emission spectra recorded in CH_3CN solutions are reported in Table III.

The emission spectra recorded in water solutions were blue shifted with respect to those observed in acetonitrile solutions, with shifts of the emission maxima on the order of $1.4 \mu m^{-1}$ for $Ru(bpy)_2(CN)_2$ and $Ru(phen)_2(CN)_2$, $0.09 \mu m^{-1}$ for (2,2) and (2,2'), and $0.04 \mu m^{-1}$ for (2,2,2).

Low-temperature emission spectra were measured in absolute ethanol glasses at 77 K. The spectra of (2,2) and (2,2,2) are reported in Figure 5 and compared with the spectrum of the $Ru(bpy)_2(CN)_2$ complex. The spectrum of (2,2') is also reported in Figure 5 and compared with those of the $Ru(bpy)_2(CN)_2$ and $Ru(phen)_2(CN)_2$ complexes. The lifetimes measured at 77 K are reported in Table III.

The excitation spectra of the (2,2), (2,2'), and (2,2,2) complexes were found to be superimposable on the absorption spectra in the UV as well as in the visible region.

No emission was observed in freshly prepared aqueous or D_2O solutions containing singly oxidized forms of the polynuclear complexes.

Discussion

Structural Considerations. The analytical and conductometric data are in good agreement with the formulation of the binuclear complexes as 1:1 electrolytes and of the trinuclear complex as a 2:1 electrolyte. The infrared spectra exhibited by the polynuclear complexes are consistent with the presence of $Ru(bpy)_2$ units in the (2,2) and (2,2,2) complexes and of $Ru(bpy)_2$ and $Ru(phen)_2$ units in the (2,2') complex. The analysis of the cyanide stretching region provides some structural information. Bridging cyano groups have been generally observed to absorb at higher frequencies with respect to terminal cyano groups.^{43,57,58} Coordination of one or two metal units to the nitrogen end of cyanide

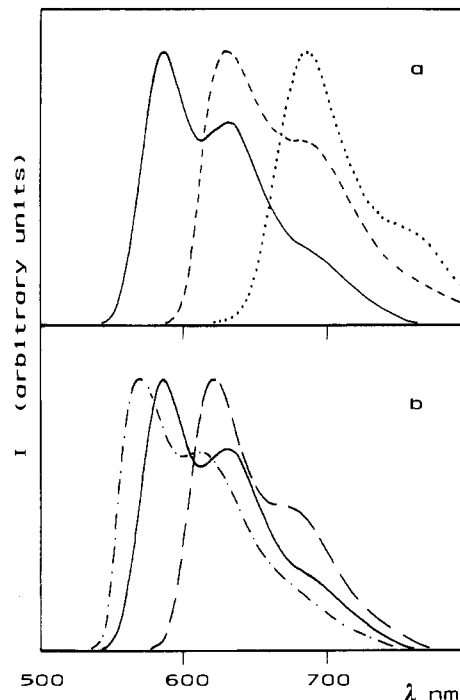


Figure 5. Low-temperature (77 K) emission spectra in absolute ethanol glass: (a) $Ru(bpy)_2(CN)_2$ (—), $[NC-Ru(bpy)_2-CN-Ru(bpy)_2-CN](PF_6)$ (---), $[NC-Ru(bpy)_2-CN-Ru(bpy)_2-NC-Ru(bpy)_2-CN](PF_6)_2$ (···); (b) $Ru(phen)_2(CN)_2$ (---), $Ru(bpy)_2(CN)_2$ (—), $[NC-Ru(bpy)_2-CN-Ru(phen)_2-CN](PF_6)$ (---).

in $Ru(bpy)_2(CN)_2$ has been observed to shift one or both of the CN bands at higher energy, with shifts on the order of $40-60 cm^{-1}$ (see Ru-Pt adducts in Table I).²² The polynuclear complexes show well-defined doublets in the CN region. By comparison of the frequencies of the CN bands of (2,2), (2,2'), and (2,2,2) with those of the mono- and dicyano mononuclear ruthenium complexes (Table I), it can be seen that one band is in the frequency range of terminal cyanide groups and the other (at higher energy) is in that of the bridging ones. The relative intensities of the bands in the doublets (Table I) confirm the presence of a greater number of bridging cyanides for the trinuclear complex than for the binuclear one. The above observation are all consistent with the formulations given for the bi- and trinuclear complexes: $NC-Ru^{II}(bpy)_2-CN-Ru^{II}(bpy)_2-CN^+$; $NC-Ru^{II}(bpy)_2-CN-Ru^{II}(phen)_2-CN^+$; $NC-Ru^{II}(bpy)_2-CN-Ru^{II}(bpy)_2-NC-Ru^{II}(bpy)_2-CN^{2+}$.

For the $NC-Ru^{II}(bpy)_2-CN-Ru^{II}(phen)_2-CN^+$ and $NC-Ru^{II}(bpy)_2-CN-Ru^{II}(bpy)_2-NC-Ru^{II}(bpy)_2-CN^{2+}$ complexes, the bonding mode of the bridging cyanides is determined by the synthetic procedure used (see the Experimental Section), assuming that no linkage isomerization occurs during the reaction. For $NC-Ru^{II}(bpy)_2-CN-Ru^{II}(bpy)_2-NC-Ru^{II}(bpy)_2-CN^{2+}$, this assumption is supported by the electrochemical results (see the next section).

The left and right symbols as used in the abbreviations (2,2) and (2,2') will hereinafter be used to designate the C-bonded and N-bonded ruthenium atoms respectively. In the trinuclear complex, (2,2,2), the central symbol will refer to the N,N-bonded $Ru(bpy)_2$ unit.

As far as the molecular structure is concerned, given the cis geometry of each $-Ru(bpy)_2-$ unit,^{59,60} several conformations are possible for all these molecules following rotation about the bridging cyanide(s). Some insight into these conformational possibilities can be gained by inspection of CPK space-filling models, in which various combinations of Λ or Δ absolute con-

(57) Dows, D. A.; Haim, A.; Wilmarth, W. K. *J. Inorg. Nucl. Chem.* **1961**, *21*, 37.

(58) Shriver, D. F. *J. Am. Chem. Soc.* **1963**, *85*, 1405.

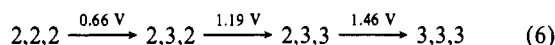
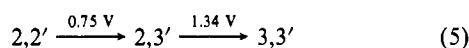
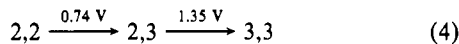
(59) The fact that the $-CN-Ru(bpy)_2-NC-$ unit (for which no structural data are obviously available as a mononuclear species) also prefers the cis configuration is demonstrated by the X-ray structure of the trinuclear complex $NC-Cr(cyclam)-CN-Ru(bpy)_2-NC-Cr(cyclam)-CN^{4+}$.⁶⁰

(60) Bertolasi, V. Private communication.

figurations of the chiral $-\text{Ru}(\text{bpy})_2-$ group are examined. For the binuclear complexes, this approach suggests that, whatever may be the chirality at ruthenium centers, rotation of $\text{Ru}(\text{bpy})_2$ units around the bridging cyanide is relatively free. The only restrictions are for the trans (Δ, Δ) or (Δ, Δ) (with respect to terminal cyanides) and cis (Δ, Δ) planar configurations, which are unfavored by steric hindrance between the polypyridine ligands. For the trinuclear complex, a greater hindrance to rotation of $\text{Ru}(\text{bpy})_2$ units around the two bridging cyanides is found, and a configuration with coplanar bridging and terminal cyanides in an all-cis geometry seems to be largely favored.

Redox Properties. In the electrochemical behavior of the mononuclear and polynuclear complexes, the following features are evident: (i) the number of one-electron-oxidative processes corresponds to the number of ruthenium atoms in the complexes; (ii) the first oxidation potential $E_{1/2}^{\text{ox}}(1)$ decreases in going from the mononuclear to the polynuclear complexes. The assignment of the redox sites that are involved in such processes requires the examination of the electrochemical data reported in Table II. The cathodic shift of the first oxidation potential in the series $\text{Ru}(\text{bpy})_2(\text{CN})_2$, (2,2), and (2,2,2) indicates that the ease of oxidation of the ruthenium atom increases in the order NC-Ru-CN , NC-Ru-NC , and CN-Ru-NC , in agreement with the ammonia-like character of N-bonded cyanide. The same conclusion can be drawn if the $E_{1/2}^{\text{ox}}(1)$ value of the (2,2') complex, in which the $-\text{Ru}(\text{phen})_2-\text{CN}$ unit is N-bonded to the bridging cyanide, is compared with that of the $\text{Ru}(\text{phen})_2(\text{CN})_2$.

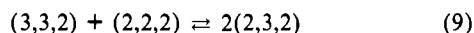
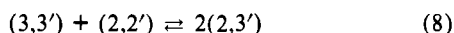
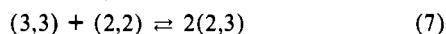
The $E_{1/2}$ data reported in Table II are therefore assigned to the following processes:



The separation between the potentials for the second and the third oxidation steps of the trinuclear complex (i.e., for oxidation of the two equivalent terminal Ru(II) sites) is 0.27 V, a figure that seems to be quite high for a symmetric system.⁶¹ The reasons for this high value should be looked for in the various factors that are known to affect the comproportionation constant of symmetric mixed-valence species.⁶²⁻⁶⁴ Among these, electron delocalization, which is present to a relatively large extent in these systems (see next section), could be considered as a significant contributor to the observed potential separation.

The separation between the potentials for the first and the second oxidation steps in both the trinuclear and binuclear systems is much larger (0.5–0.6 V, respectively). This can be obviously justified on the basis of the redox asymmetry of the metal centers involved, which in turn arises from the asymmetry of the bridging cyanide. On the basis of the relatively small shifts between the MLCT bands of different units in the fully reduced forms of these systems, this redox asymmetry should not contribute more than ca. 0.2–0.3 V to the potential separation. The remaining part is again attributable to other factors, such as electron delocalization through the cyanide bridges.

The K_c constants of the comproportionation equilibria shown in eq 7–9, estimated from $E_{1/2}$ values, are on the order of 10^{10}



for the binuclear complexes and 10^9 for the trinuclear. These

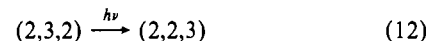
values indicate that the one-electron oxidation of (2,2), (2,2'), and (2,2,2) quantitatively gives the (2,3), (2,3'), and (2,3,2) mixed-valence species.

Spectroscopic Properties. The proportional increase in the visible absorption intensity in going from monomeric to trimeric complexes, shown in Figure 2, agrees with the presence of several closely spaced (Ru–bpy) CT transitions originating in the C-bonded and N-bonded ruthenium atoms of the $\text{Ru}(\text{bpy})_2$ cyano-bridged units.

The solvatochromic behavior exhibited by the (2,2), (2,2'), and (2,2,2) complexes in going from acetonitrile to water (see Figure 2 vs Figure 4) can largely be assigned to hydrogen bonding effects operating at the terminal cyanide groups.^{22,54-56} In these terms, the structured visible absorption shown by the (2,2,2) complex in water or D_2O solutions (see Figure 4) can be rationalized. The shoulder at ca. $2 \mu\text{m}^{-1}$ can be assigned to $d-\pi^*$ transitions localized on the central $-\text{CN-Ru}(\text{bpy})_2-\text{NC}-$ unit, while the more intense band at $2.3 \mu\text{m}^{-1}$ should arise from $d-\pi^*$ transitions localized on the two terminal $\text{NC-Ru}(\text{bpy})_2-\text{CN}-$ units, more exposed to second-sphere interactions.

The oxidation of the (2,2), (2,2'), and (2,2,2) complexes gives rise to a blue shift and a decrease of the intensity of the absorption bands in the visible region and to the formation of a new absorption band in the near-infrared region. The spectra in D_2O solutions of the reduced and one-electron-oxidized forms of the polynuclear complexes are reported in Figure 4. The residual absorptions in the visible region, shown by the oxidized species, are assigned to ($d-\pi^*$) CT transitions localized on the $-\text{NCRu}^{\text{II}}(\text{bpy})_2\text{CN}$ units. The shifts at higher energy of these bands upon oxidation of attached metal-containing units have been previously discussed for other polynuclear systems based on the $\text{Ru}(\text{bpy})_2(\text{CN})_2$ unit.^{9,10}

The new bands in the near-infrared region can be confidently assigned to the following metal-to-metal IT transitions:⁶⁵⁻⁶⁷



The parameters (molar absorptivity, energy, and half-width of the IT bands) can be used to calculate, according to the Hush model,⁶⁸ the electronic interaction matrix elements H_{AB} and the degree of delocalization α^2 between adjacent metal centers in these mixed-valence complexes. Taking a typical metal-metal distance of 5 Å, the values for $\text{NC-Ru}^{\text{II}}(\text{bpy})_2-\text{CN-Ru}^{\text{III}}(\text{bpy})_2-\text{CN}^{2+}$ are $H_{AB} = 0.2 \mu\text{m}^{-1}$ and $\alpha^2 = 0.07$.

Similar values are obtained for the other complexes. A comparison between the electronic interaction and the energy of the IT transition ($0.89 \mu\text{m}^{-1}$) places $\text{NC-Ru}^{\text{II}}(\text{bpy})_2-\text{CN-Ru}^{\text{III}}(\text{bpy})_2-\text{CN}^{2+}$ (as well as the other complexes studied) somewhat beyond the borderline defining class II mixed-valence complexes ($2H_{AB} \ll \text{optical energy}$) though still far from the true class III domain ($2H_{AB} = \text{optical energy}$).^{62,69,70} Moreover, the IT bands

(65) It can be noticed that the IT band of the trinuclear complex in Figure 4 has a distinct shoulder on the high-energy side, shifted by ca. $0.3 \mu\text{m}^{-1}$ with respect to the maximum. The shoulder certainly belongs to the same IT transition as the band maximum, since the whole band grows up with rigorously constant band profile upon electrochemical oxidation, irrespective of the potential applied within the whole range of the first oxidation wave. The splitting of the IT band seems to be too large to be attributed to spin-orbit coupling, if it is compared with that (ca. $0.48 \mu\text{m}^{-1}$) observed by Kober et al. in the case of heavier Os(II)–Os(III) systems.⁶⁶ An example of multiple IT bands in a Ru(II)–Ru(III) system has been recently reported by Ludi,⁶⁷ although a simple explanation for the observed splittings was not given.

(66) Kober, E. M.; Goldsby, K. A.; Narayana, D. N. S.; Meyer, T. J. *J. Am. Chem. Soc.* **1983**, *105*, 4303.

(67) Joss, S.; Bürgi, H. B.; Ludi, A. *Inorg. Chem.* **1985**, *24*, 949.

(68) Hush, N. S. *Prog. Inorg. Chem.* **1967**, *8*, 391.

(69) The same conclusion, although with somewhat smaller delocalization parameters, had been previously reached for other cyano-bridged complexes.^{9,10,70}

(70) Glauser, R.; Hauser, U.; Herren, F.; Ludi, A.; Roder, P.; Schmidt, E.; Siengenthaler, H.; Wenk, F. *J. Am. Chem. Soc.* **1973**, *95*, 8457.

(61) For comparison, it may be recalled that the separation in the case of the oxidation of two equivalent terminal Ru(II) sites of $\text{Ru}(\text{NH}_3)_5-\text{NC-Ru}(\text{bpy})_2-\text{CN-Ru}(\text{NH}_3)_5^{4+}$ is 0.07 V.⁹

(62) Creutz, C. *Prog. Inorg. Chem.* **1983**, *30*, 1 and references therein.

(63) Richardson, D. E.; Taube, H. *Coord. Chem. Rev.* **1984**, *60*, 107.

(64) Goldsby, K. A.; Meyer, T. J. *Inorg. Chem.* **1984**, *23*, 3002.

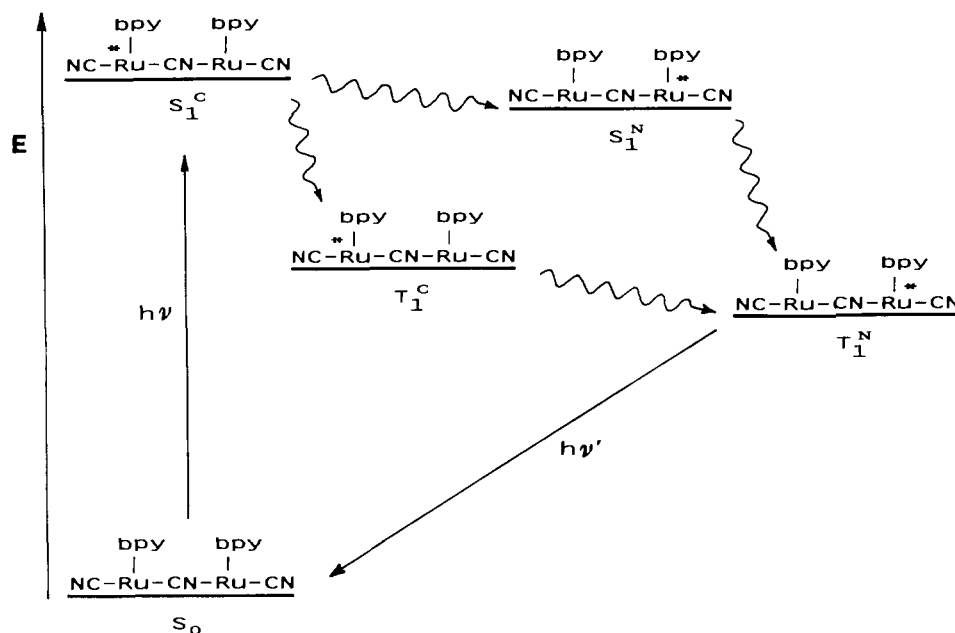


Figure 6. Schematic representation of the radiative and radiationless processes that can occur upon excitation of $\text{NC-Ru}^{\text{II}}(\text{bpy})_2\text{-CN-Ru}^{\text{II}}(\text{bpy})_2\text{-CN}^+$.

are appreciably Gaussian-shaped and have half-widths (ca. $0.35 \mu\text{m}^{-1}$) that are consistent with class II behavior. From a practical point of view, therefore, allowing for some quantitative deviation from ideality, these complexes can be considered as essentially valence-localized species. This approach has been and will be followed in the discussion of electrochemical properties, absorption and emission spectra, and photophysical behavior.

Photophysical Properties. Contrary to what happens in the model polynuclear complexes of the type $\text{Ru}(\text{bpy})_2(\text{CN})_2(\text{X})_{1,2}$ ($\text{X} = \text{Pt}(\text{II}),^{22} \text{Zn}(\text{II}),^{71} \text{Ag}(\text{I}),^{20} \text{Cu}(\text{I})^{71}$) the room-temperature (see Table III) and 77 K emission (see Figure 5) of the (2,2) and (2,2,2) complexes are progressively red-shifted with respect to that of the $\text{Ru}(\text{bpy})_2(\text{CN})_2$ complex. The same behavior is exhibited by the (2,2') binuclear complex with respect to the $\text{Ru}(\text{bpy})_2(\text{CN})_2$ and $\text{Ru}(\text{phen})_2(\text{CN})_2$ complexes (see Table III and Figure 5). On the basis of the observed trend in the oxidation potentials, it was suggested that the ease of oxidation of the Ru centers increases in the series NC-Ru-CN , CN-Ru-CN , CN-Ru-NC ; thus, the lowest $d-\pi^*$ excited state in each complex should be localized on the Ru center with the greater number of N-bonded cyanides. Consistent with this hypothesis are the bathochromic shift and the less pronounced solvent dependence of the emissions, observed in going from $\text{Ru}(\text{bpy})_2(\text{CN})_2$ to (2,2) and (2,2,2). This conclusion is further strengthened by the behavior of the (2,2') complex in which the CN-Ru-CN unit has the phenanthroline ligand instead of bipyridine. The long emission lifetime characteristic of the phenanthroline complexes (see lifetimes in Table III) labels the emitting state as belonging to the CN-Ru-CN unit.

For all these bi- and trinuclear species, the perfect agreement between excitation and absorption spectra indicates that intramolecular energy transfer from the higher chromophoric unit(s) to the lowest emitting one, as depicted in Figure 6 for the (2,2) complex, occurs with unitary efficiency. In Figure 6, both of the possible spin-allowed exergonic energy-transfer processes, i.e. singlet-singlet and triplet-triplet, are considered. In similar bimolecular energy transfer processes, only the triplet pathway, proceeding by an exchange mechanism, would be usually considered due to the very short lifetime of the singlet MLCT state of $\text{Ru}(\text{II})$ polypyridine complexes.⁷² In these polynuclear systems, however, the possibility of a very rapid singlet-singlet transfer via a dipole-dipole mechanism cannot in principle be ruled out. An alternative mechanism such as the triplet-singlet Forster-type transfer proposed by Furue¹⁶ for methylene-bridged $\text{Ru}(\text{II})/\text{Os}(\text{II})$ polypyridine complexes is not expected to be efficient in these

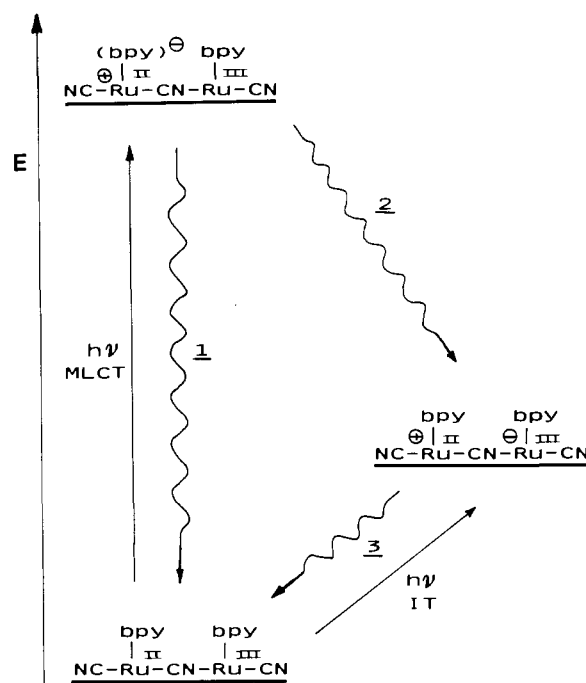


Figure 7. Schematic representation of the intramolecular electron-transfer quenching processes of the $d-\pi^*$ excited state of $\text{NC-Ru}^{\text{II}}(\text{bpy})_2\text{-CN-Ru}^{\text{III}}(\text{bpy})_2\text{-CN}^{2+}$.

systems due to very poor overlap between phosphorescence and absorption spectra.

The one-electron-oxidized forms of the bi- and trinuclear complexes (2,3), (2,3'), and (2,3,2) do not emit. As previously observed in other related mixed-valence complexes based on the $\text{Ru}(\text{bpy})_2(\text{CN})_2$ chromophoric unit,^{9,10} the main quenching pathway can be assigned to highly efficient intramolecular electron transfer. As an example, for the binuclear complex (2,3), the main quenching pathway of the ($d-\pi^*$) excited state of the $\text{Ru}(\text{bpy})_2^{2+}$ chromophore can be represented as in Figure 7. In terms of standard electron transfer models, the interfragment quenching (step 2) is expected to be faster than the usual intrafragment excited state deactivation (step 1). In fact, both steps are highly exergonic and most probably lie in the Marcus inverted region.⁷³ Step 2 is, however, less exergonic and involves a larger reorgan-

(71) Bignozzi, C. A. Unpublished results.

(72) Watts, R. J. *J. Chem. Educ.* **1983**, *60*, 834.

(73) Marcus, R. A. *Annu. Rev. Phys. Chem.* **1964**, *15*, 155.

izational energy than step 1 and is thus expected to be faster.

No appreciable transient absorption changes ($\tau \geq 30$ ns) are observed in laser flash photolysis of the one-electron-oxidized forms. It should be remarked that the spectra of intermediates of the type of that shown in Figure 7 are expected to be similar (except for small shifts on the order of 0.1–0.2 μm^{-1}) to those of the corresponding ground states. The most plausible explanation of the observed lack of spectral changes, however, is that the charge recombination (step 3), despite of the low exergonicity, is in the nanosecond or subnanosecond range. This conclusion is consistent with the kinetic parameters for the back-recombination reaction (step 3) that can be estimated from the spectral characteristics of the IT bands.^{62,74}

Conclusions

It has been shown that the stepwise synthesis of discrete oligomeric complexes containing $\text{Ru}(\text{bpy})_2^{2+}$ chromophoric units linked together by cyanide bridges is feasible. These complexes can be considered as pseudohomopolynuclear, in the sense that they are made up of identical building blocks connected, however, by asymmetric bridges. Indeed, their behavior is deeply influenced by the asymmetry of the bridges connecting the chromophoric units. In particular, it has been shown that (i) the more easily

oxidizable Ru(II) centers in the polynuclear complexes are those that contain the greater number of N-bonded cyanides, (ii) the lowest MLCT excited state is always localized on the $\text{Ru}(\text{bpy})_2^{2+}$ unit that has the greater number of N-bonded cyanides, and (iii) very efficient intramolecular energy transfer takes place from all the $\text{Ru}(\text{bpy})_2^{2+}$ chromophoric units to that having the lowest excited state. Partial oxidation of these species gives rise to strong intervalence bands in the near-infrared region, indicating a relatively large degree of electron delocalization (relative to typical class II mixed-valence behavior).

These results are of some general interest, in particular with regard to the synthesis and the properties of more extended, polymeric structures of the same type. The possibility to direct intramolecular energy and electron transfer by taking advantage of the asymmetry in the bridging ligands seems to be particularly interesting in this regard.

Acknowledgment. This work was supported by the Ministero della Pubblica Istruzione and by the Consiglio Nazionale delle Ricerche (Progetto Finalizzato Chimica Fine e Secondaria II).

Registry No. (2,2)PF₆, 123165-05-9; (2,2')PF₆, 123099-59-2; (2,2,2)(PF₆)₂, 123099-63-8; (2,3)(PF₆)₂, 123099-65-0; (2,3')(PF₆)₂, 123099-67-2; (2,3,2)(PF₆)₃, 123099-69-4; $\text{Ru}(\text{bpy})_2(\text{NO}_2)(\text{CN})$, 123099-54-7; $\text{Ru}(\text{phen})_2(\text{NO}_2)(\text{CN})$, 123099-55-8; $[\text{Ru}(\text{phen})_2(\text{NO})(\text{NO}_2)](\text{PF}_6)_2$, 31450-89-2; $[\text{Ru}(\text{bpy})_2(\text{NO})(\text{CN})](\text{PF}_6)_2$, 121176-17-8; $[\text{Ru}(\text{phen})_2(\text{NO})(\text{CN})](\text{PF}_6)_2$, 123099-57-0; $\text{Ru}(\text{bpy})_2(\text{CN})_2$, 20506-36-9; $[\text{Ru}(\text{phen})_2(\text{CH}_3\text{OH})(\text{CN})]\text{PF}_6$, 123099-61-6; $\text{Ru}(\text{bpy})_2\text{Cl}_2$, 19542-80-4; $\text{Ru}(\text{phen})_2(\text{CN})$, 112087-85-1; $[\text{NCRu}(\text{bpy})_2\text{CNPt}(\text{dien})](\text{ClO}_4)_2$, 88360-14-9; $[(\text{dien})\text{PtNCRu}(\text{bpy})_2\text{CNPt}(\text{dien})](\text{ClO}_4)_4$, 88377-85-9; $\text{Ru}(\text{bpy})_2(\text{CH}_3\text{OH})(\text{NO}_2)^+$, 47637-64-9.

(74) For example, using $\epsilon_{\text{max}} = 10\,000 \text{ M}^{-1} \text{ cm}^{-1}$, $\nu_{\text{max}} = 0.80 \mu\text{m}^{-1}$, and $\Delta\nu_{1/2} = 0.35 \mu\text{m}^{-1}$ as experimental spectroscopic parameters, $\Delta G = 0.25 \text{ eV}$ as a reasonable driving force value and $\nu_N = 1 \times 10^{10} \text{ s}^{-1}$ as a plausible (mainly outer-sphere) frequency factor, one obtains from standard equations⁶² a calculated rate constant value of $4 \times 10^{10} \text{ s}^{-1}$ for the back-recombination step in the mixed-valence binuclear complexes.

Contribution from the Department of Chemistry and Biochemistry,
University of California, Los Angeles, California 90024

Quantitative Evaluation of the Relationships between Excited-State Geometry and the Intensities of Fundamentals, Overtones, and Combination Bands in Resonance Raman Spectra

Kyeong-Sook Kim Shin and Jeffrey I. Zink*

Received February 14, 1989

The factors that govern the resonance Raman intensities of fundamentals, overtones, and combination bands are quantitatively evaluated. The calculations and interpretation are based on the time-dependent theory of Lee, Tannor, and Heller. From the time-dependent point of view, the Raman intensities are governed by the overlap of the time-dependent wave packet with the final Raman wave function of interest as a function of time. The most important factors are the magnitude of the overlap and the time development of the overlap. The magnitudes of the overlaps for overtones of a given mode are smaller than that for its fundamental, and the magnitude for a combination band is smaller than those of the fundamentals of the modes comprising the combination band. Thus, the overtone and combination bands are weaker than fundamentals. The time development of the overlap depends on both the frequency of the vibration and the displacement of the excited potential surface relative to the ground potential surface along the normal coordinate. The damping of the overlap determines whether short-time or long-time processes dominate the intensities. For large molecules where short-time processes dominate, the larger the initial overlap and the faster the overlap increases with time, the higher the Raman intensity. The intensities of fundamentals, overtone bands, and combination bands will be discussed in terms of the overlap. Qualitative rules for interpreting excited-state molecular properties from the Raman intensities are developed. The spectra of $\text{W}(\text{CO})_5(\text{pyridine})$ and $\text{Rh}_2(\text{O}_2\text{CCH}_3)_4\text{L}_2$, where $\text{L} = \text{PPh}_3$ or AsPh_3 , are analyzed.

1. Introduction

Resonance Raman spectroscopy is frequently considered to be a complicated and esoteric method of obtaining vibrational spectra. However, the time-dependent theory of Lee, Tannor, and Heller shows that it is closely akin to absorption spectroscopy.¹⁻⁴ In addition, the new point of view shows that the intensity of a peak

in a Raman spectrum provides detailed information about the excited-state potential surface along the normal mode giving rise to the peak.⁵⁻⁸

The purpose of this paper is to examine resonance Raman intensities from the time-dependent theoretical point of view in order to state general, qualitative rules for interpreting excited-state

(1) Lee, S.-Y.; Heller, E. J. *J. Chem. Phys.* **1979**, *71*, 4777.
(2) Heller, E. J. *Acc. Chem. Res.* **1981**, *14*, 368.
(3) Heller, E. J.; Sundberg, R. L.; Tannor, D. J. *Phys. Chem.* **1982**, *86*, 1822.
(4) Tannor, D.; Heller, E. J. *J. Chem. Phys.* **1982**, *77*, 202.

(5) Williams, S. O.; Imre, D. G. *J. Phys. Chem.* **1988**, *92*, 3363.
(6) Yoo, C. S.; Zink, J. I. *Inorg. Chem.* **1983**, *22*, 2474.
(7) Yang, Y. Y.; Zink, J. I. *Inorg. Chem.* **1985**, *24*, 4012.
(8) Myers, A. B.; Mathies, R. A.; Tannor, D. J.; Heller, E. J. *J. Chem. Phys.* **1982**, *77*, 3857.